



HORIZON-CL5-2023-D3-02-12
Large area perovskite solar cells and modules

LUMINOSITY

Large area uniform industry compatible perovskite solar cell technology

Starting date of the project: 01/06/2024
Duration: 48 months

= Deliverable D3.2 = **Specifications for transport layers for upscaled processing**

Dissemination level		
PU	Public	X
SE	Sensitive, limited under the conditions of the Grant Agreement	
Classified R-UE/EU-R	EU RESTRICTED under the Commission Decision No2015/444	
Classified C-UE/EU-C	EU CONFIDENTIAL under the Commission Decision No2015/444	
Classified S-UE/EU-S	EU SECRET under the Commission Decision No2015/444	



This project has received funding from the European Union's Horizon Europe research and innovation programme under grant agreement No 101147653.

Views and opinions expressed are those of the author(s) only and do not necessarily reflect those of the European Union or European Commission. Neither the European Union nor the granting authority can be held responsible for them.

Executive Summary

This deliverable summarizes the preliminary specifications for the transport layers and reflects these on feasibility and resulting specifications for later industrial upscaling.

It is closely coupled to Deliverable 1.1 Blueprint of R2R processing line.

Table of Contents

1. Introduction	5
2. Hole transport layer	5
2.1. <i>NiOx as hole transport layer.....</i>	<i>5</i>
2.2. <i>Alternative materials as HTL.....</i>	<i>6</i>
3. Electron transport layer and buffer layers	6
3.1. <i>Fullerene interlayers as high-performance diffusion blocking layers.....</i>	<i>8</i>
3.2. <i>Buffer layer.....</i>	<i>8</i>
3.3. <i>Soft-sputtered SnO2 for ETL and buffer layers.....</i>	<i>10</i>
3.4. <i>Soft sputtering of In-free TCO.....</i>	<i>11</i>
4. Conclusions.....	15
5. Degree of Progress.....	15
6. Dissemination level.....	15

1. Introduction

The deliverable discusses the various aspects and specifications for transport layers for upscaled processing of perovskite cell and modules. It reflects the knowledge in month 6 of the LUMINOSITY project.

Transport layers in perovskite solar cells play a crucial role in enhancing their efficiency and stability. These layers are typically composed of materials that facilitate the movement of charge carriers (electrons and holes) generated in the perovskite absorber layer when exposed to light. The transport layers must possess high conductivity, good energy level alignment with the perovskite layer, and adequate transparency to allow light to reach the absorber. The optimization of these transport layers is essential for minimizing recombination losses and improving the overall performance of perovskite solar cells.

2. Hole transport layer

2.1. NiOx as hole transport layer

NiOx is selected as a robust and efficient hole transport layer (HTL) to be used in perovskite solar cells and modules in LUMINOSITY. A suitable NiOx as an HTL should have good conductivity ($<10 \text{ k}\Omega\text{cm}$), low absorbance in the absorption range of perovskite absorber ($< 8\%$ in the range 400-800 nm), act as a diffusion barrier against ion migration, and display long-term stability (at room temperature, and at elevated temperature stress tests, 85 °C).

TNO has recently started developing the process for NiOx sputtering in a S2S sputtering tool. The development of NiOx sputtering will be done with a view of obtaining the correct stoichiometry for the best hole conductivity. For this, a start is made with a reactive sputtering process in which processing parameters, such as working pressure, oxygen partial pressure and power will be screened. The first aim is to obtain the best NiO HTL regardless of the requirements of low temperature post-processing, thanks to high temperature resistance of Al foil. However, for the speed, and CO2 footprint of the process, it is desirable to find a process parameter space which allows deposition of NiO up to specifications without any high temperature post treatment.

The use of NiOx which is now classified as CMR material (carcinogenic, mutagenic and toxic to reproduction) presents us with major challenges in terms of health protection, which must be solved responsibly and economically within the project. In this context a potential alternative approach is solution processing of NiOx. The solution processing is potentially a lower risk alternative to sputtering, as there is no vapor of NiOx precursors that needs to be kept under control.

NiOx can be deposited in a solution process, where the precursors of NiOx (usually from nickel nitrates) are dissolved in suitable (co-)solvent systems. The state of the art processing of NiOx from solution processed layers is to dissolve nickel nitrate in 2-methoxy ethanol (2ME). By adding a small amount of acetylacetonate (AcAc) as a catalyst, the conversion temperature for the desired oxidation state is reduced down to 300°C. TNO has experience depositing solution processed pristine and doped NiOx layers (such as Cu:NiOx) using 2ME:AcAc solvent-catalyst system. However, 2ME is a highly toxic, and carcinogenic solvent, which cannot be used in ambient R2R processing. TNO will look for alternative solvent systems, that will replace the toxic 2ME with R2R coatable counterparts. To counteract the use of toxic solvents, Empa has developed solution processed NiOx with ethanol based solvent system. Blade-coating was used as the method of deposition and the NiOx NP was passivated at the top using blade-coated SAMs. The fully solution processed scalable bilayer HTL stack showcase excellent uniformity and comparable peak performance to the standalone SAM based devices.

2.2. Alternative materials as HTL

TNO has been working on R2R slot-die coatable HTLs since several years. One of the most common HTL that is deposited during R2R slot-die coating is PTAA polymer. Once considered very expensive, PTAA polymer is now a relatively cheap option if bought in sufficiently large amounts. The increasing demand on this polymer also resulted in many companies producing this polymer in large quantities (grams), which in turn reduced the market price more than a decade with respect to producers that selling for a small amount (milligrams). Furthermore, PTAA is known as an efficient, low temperature process material. However, the stability of this layer needs to be further assessed. Another alternative is a group of materials that are called self-assembled monolayers (SAMs). SAMs has been in the focus of researchers, first in combination with NiOx as a bilayer HTL, and then later as a stand-alone HTL. SAMs consist of a head group and a functional group, which assembles on an oxide surface, such as ITO, FTO, NiOx, and works as a hole-selective contact. SAMs can be dissolved in alcohols, which are suitable for R2R processing. As alternative, TNO can potentially focus on R2R deposition of SAMs as suitable HTLs in perovskite solar cell stacks. First indications from within the LUMINOSITY partners and from the literature show that SAMs can be efficient and potentially stable. Empa has been screening alternative HTLs such as Antimony doped Tin oxide (ATO) using spin-coating method. From the initial trials, the ATO-based device with addition of SAM HTL in a bilayer configuration showcase improved device performance compared to NiO/SAM bilayer based perovskite solar cells. Further efforts to upscale the ATO HTL with scalable methods will be devoted to achieve non-toxic fully scalable HTL stack.

3. Electron transport layer and buffer layers

The upscalability of hybrid organic-inorganic perovskite solar module process demands compact and high-performance solution-based Electron Transporting Layers (ETLs) and buffer layers/interlayers.

3.1. Fullerene interlayers as high-performance ETLs and diffusion blocking layers

Fullerene layers are deposited on top of the perovskite absorber, enabling electron extraction and also enabling the deposition of the buffer layer (nanoparticle SnO₂ or ALD-SnO₂) on itself. There has been several attempts to deposit different forms of SnO₂ directly on perovskite, however the interaction of I-species in perovskite with Sn-species resulted in failure of perovskite solar cell stack. In this aspect, fullerene layers play a critical role. Thick fullerene ETL (~200 nm) have been reported to improve the stability of MAPbI₃ based perovskite solar cells, acting as blocking layer for ion diffusion. However it negatively impact the power conversion efficiency (PCE) due to the limited conductivity of PC₇₀BM (Galatopoulos, F.; Papadas, I. T.; Armatas, G. S.; Choulis, S. A., *Adv. Mater. Interfaces* **2018**, *5*, 1800280). To address this issue, CUT has proposed that using N-DMBI as n-type dopant can improve the conductivity of PC₇₀BM. The aforementioned n-type doping with N-DMBI, in conjunction with thick fullerene buffer layer can be proven to be a viable interlayer that acts as high-performance diffusion blocking layer. Therefore, the spin-coated fabrication of perovskite solar cells with improved stability while simultaneously retaining similar PCE with the optimum reference of 70 nm PCBM can be achieved. This strategy is implemented in the LUMINOSITY project, where LUMINOSITY based fullerene interlayers and FAPbI₃ based perovskite formulations must be compatible with large scale and ambient deposition processes (S2S and R2R). Thus, the aforementioned spin-coated fabrication process was transferred to a large-scale compatible deposition technique (meniscus coating) in ambient atmosphere.

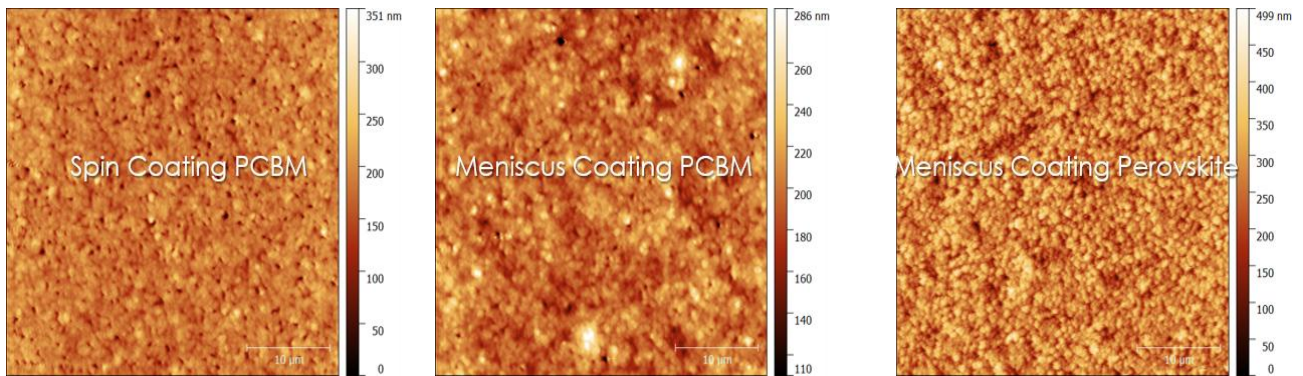


Figure 1: AFM topographical images of spin coated PCBM (left), meniscus coated PCBM (centre) and meniscus coated perovskite (right)

The initial AFM data (Figure 1) show similar morphologies between the initially reported data from spin coating and current meniscus coating deposition (roughness 25 and 17 nm respectively) with less pinholes. These results show the successful transfer of the spin coating deposition process to large scale compatible deposition techniques of the PCBM interlayer.

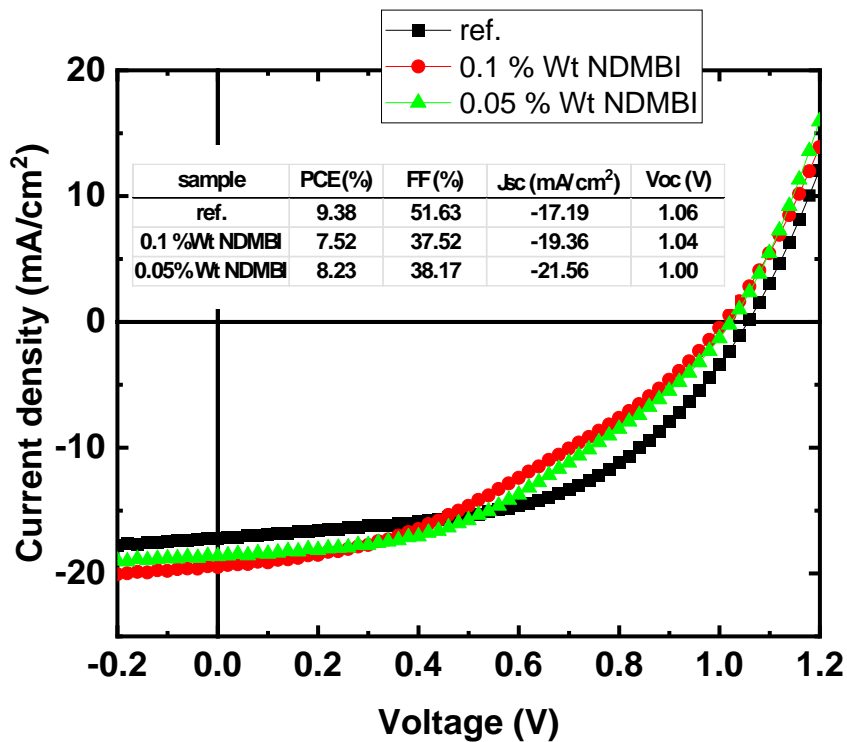


Figure 2: J/V data at 1 SUN illumination for perovskite solar cells based on pristine, 0.1 and 0.05 % N-DMBI doped PCBM.

Using meniscus coating PCBM fabrication process, solar cells were fabricated based on the ambient condition-based perovskite formulation $FAPbI_3$ to examine the compatibility of initially thin fullerene N-DMBI doped layer (70 nm) with the $FAPbI_3$ based perovskite formulation. Initial results for doping levels of 0.1 and 0.05 % are shown in Figure 2. Reference Perovskite solar cells with meniscus coating PCBM in ambient conditions delivered a champion device with PCE = 9.38%. Doping of PCBM with 0.05 % w.t. N-DMBI increases the J_{sc} from 17.19 to 21.56 mA/cm², but losses are observed in the FF and V_{oc} resulting at this stage in lower PCE.

Within the next months of the project, CUT will investigate the effect of meniscus coated N-DMBI doping on thick fullerene (~200 nm) based diffusion blocking layers using FAPbI₃ perovskite formulation aiming to achieve high performance fullerene-based ETL/diffusion blocking layers according to the requirements of the LUMINOSITY project. Furthermore, alternative n-type doping materials will be studied by CUT in order to find the appropriate material that ensures a good compromise between stability and PCE.

3.2. Protective buffer layers

To deposit Transparent Conductive Oxides (TCOs) on the top of perovskite cell and to avoid damages CNR developed a solution process buffer layer based on metal oxides nanoparticles as alternative to the SnO₂ buffer deposited with Atomic Layer Deposition (ALD). We investigated several types of metal oxides as protective buffer layers (PBLs). Nanoparticles have different metals, different solvent preparation and different sizes. These differences impact also on the electronic properties of the nanoparticles such as work function. The coating applicability of these nanoparticles encompasses spin coating, blade coating, and slot-die coating techniques, favouring a prospective upscaling. Here, the spin-coating technique was employed for the PBL deposition.

Perovskite solar cells with an inverted device configuration of glass/ITO/PTAA/PFN-Br/Cs_{0.05}MA_{0.14}FA_{0.81}PbI_{2.7}Br_{0.3}/PC61BM/PBL/ITO were employed, where solution-processed PTAA and PC61BM layers act as the hole- and electron-transport layers, respectively. The perovskite band gap is 1.6 eV. We found that the dynamically-spin-coated film could show a higher uniformity and an improved film morphology compared to static spin coating, promoting charge collection and interface extraction and resulting in a pinhole-free layer. Semitransparent cells were compared with the same stack cell but with a Cu electrode (control device). The electrical performance for different buffer layers is reported in Figure 3.

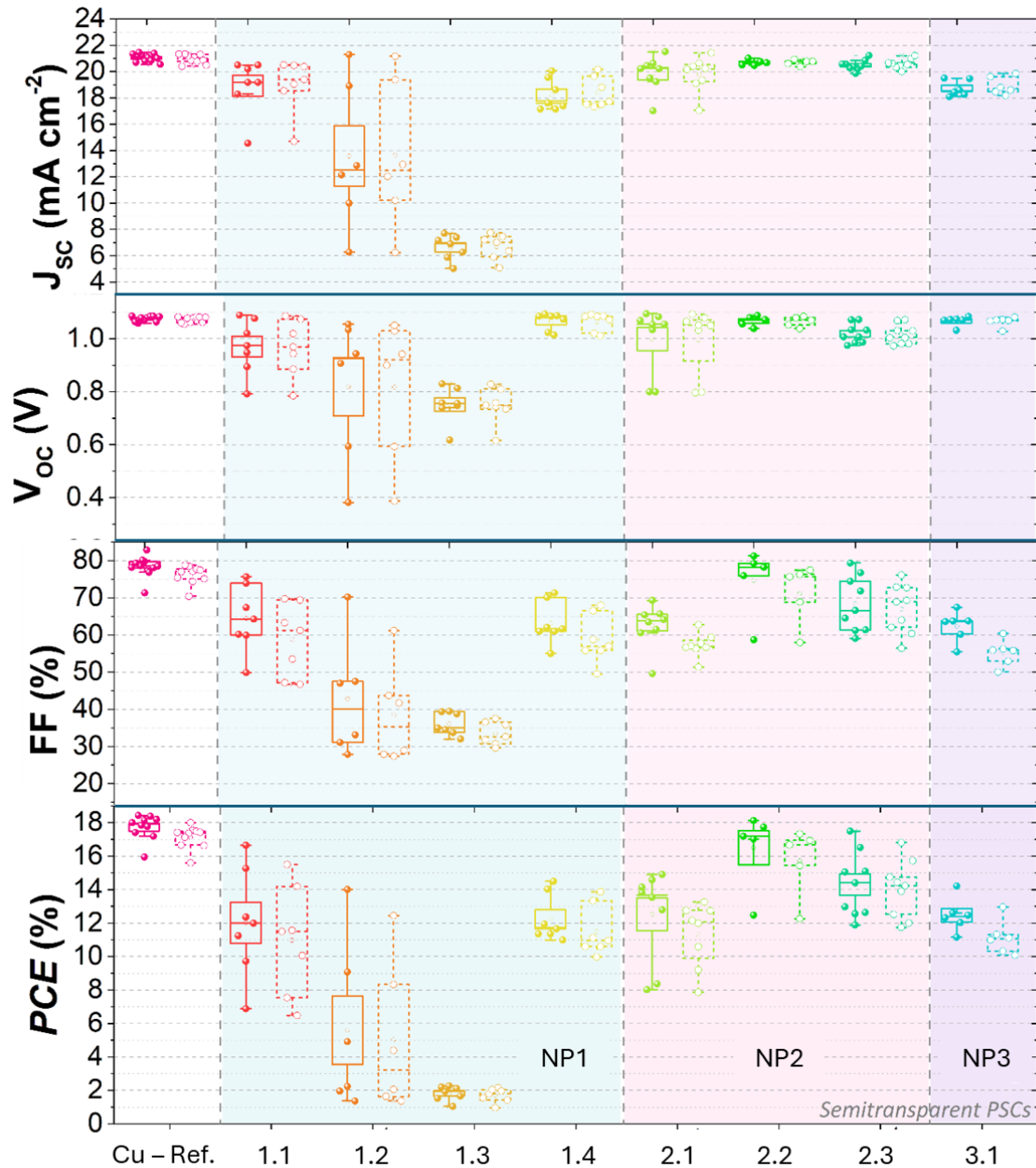


Figure 3: Comparison of the photovoltaic parameters of perovskite solar cells (glass/ITO/PTAA/Cs_{0.05}MA_{0.14}FA_{0.81}Pb I_{2.7}Br_{0.3}/PC61BM/PBL/ITO) with various solution-processed buffer layers. Both parameters measured in Forward (solid) and Reverse (dashed) tracking mode are reported. Control/Reference device have Cu electrode thermally evaporated on the perovskite cell.

Here, we do not report the ST-PSCs based on ITO/BCP (without PBL) since the J-V exhibited a significant sputtering damage, showing the typical S-shape.

As regards the NP1 PBLs, ST-PSCs based on NP1.1 showed the best performance, with a FF up to 75.7%. Nonetheless, the statistical distributions of the electrical parameters exhibited a large dispersion, indicating poor reproducibility. Similarly, a huge spread can be observed in the statistics of NP 1.2, yet with a lower efficiency. NP1.3-based ST-PSCs showed extremely reduced electrical parameters, manifesting the typical S-shape and suggesting strong sputtering damage. The best reproducibility was observed in the NP1.4-based ST-PSCs, even though poor FF and J_{sc} were measured. On the other hand, the devices based on NP1 showed poor J_{sc} and FF. NP2 PBL show a superior PCE of 18.1% for NP2.2-

based devices, close to the best opaque reference device with a PCE of 18.4%. A slightly lower performance was observed in the NP2.3 case, whereas a significant FF reduction was shown in the NP2.1-based ST-PSCs. Similar FF reduction is observed also for NP3. The superior performance of the NP2-based ST-PSCs can be attributed to a stronger resilience to sputtering damage as well as to better electrical conductivity compared to the other NPs due to the aluminum doping. Considering the superior performance and improved resilience to sputtering damage, the NP2.2 layer can be selected as optimal PBL for the semitransparent stack of the LUMINOSITY project as alternative to ALD deposited PBL.

3.3. Soft-sputtered SnO₂ for ETL and buffer layers

For the deposition of SnO₂ coatings various coating methods are available. The main challenge in this project is to establish a process that minimises the generation of defects in the underlying perovskite layer. Because the perovskite layers are sensitive to ambient air, it is advisable to handle consistently the coated samples in an inert atmosphere such as N₂ or Ar. Furthermore, the coating process must fulfil economic aspects and enable a sufficient deposition rate. At FhG FEP various vacuum based coating methods are available with various aspects, listed and evaluated in Table 1. Among the processes named in Table 1, the anodic arc evaporation is the most promising and is to be investigated and qualified for the deposition of SnO₂ layers. For anodic arc evaporation a plasma-assisted deposition using an anodic vacuum arc discharge to a tubular crucible and a hollow cathode arc plasma source is applied (Figure 4-a). At FhG FEP a novel evaporation module with material feeding was developed and built for this purpose [Scheffel et al., [Thin Solid Films, 731 \(2021\) 138731](#)]. The process is characterized by a high degree of vapor ionization (>50%), yet the energy of the vapor particles is low, which considerably reduces damage to sensitive layers already present on the substrate. The process was able to be successfully tested with indium tin oxide, indium zinc oxide, and aluminum-doped zinc oxide. To apply this method for the deposition of SnO₂ layers, some challenges have to be overcome related to its low electrical conductivity. Contrary to the tested materials up to now, it is not possible to guide the current of the vacuum arc discharge directly via the SnO₂ material to reach a direct heating and evaporation. As a compromise, the design of the evaporation unit was revised (Figure 4-b) and a new tubular crucible with conducting elements was manufactured. The next action items refer to the purchasing of SnO₂ feedstock material in the form of pressed cylindrical shaped parts, the installation and commissioning of the equipment into a suitable vacuum tool, followed by carrying out coating experiments and sampling of prepared substrate material.

Table 1: Aspects of various coating methods available at FhG FEP

Parameter	EB-PVD ¹	Soft-Sputtering	Anodic Arc Evaporation
Energy of vapor particles	~0.1 eV	~50-200 eV	~10-50 eV
Potential damage mechanisms	X-Rays, heat load, backscattered electrons	High energy particle bombardment, UV	UV
Deposition rate	~10 000 nm*m/min ~500 nm/s	~10 nm*m/min ~1 nm/s	~300-500 nm*m/min ~15 nm/s
TRL	5	6	3
Remark	low surface mobility of the adatoms results in bad layer quality	uneconomic processes due to reduced coating rates, remaining risk for the generation of defects.	high proportion of ionized particles at moderately high energies, economical attractive deposition rate, low TRL

¹ EB-PVD – Electron Beam Physical Vapor Deposition

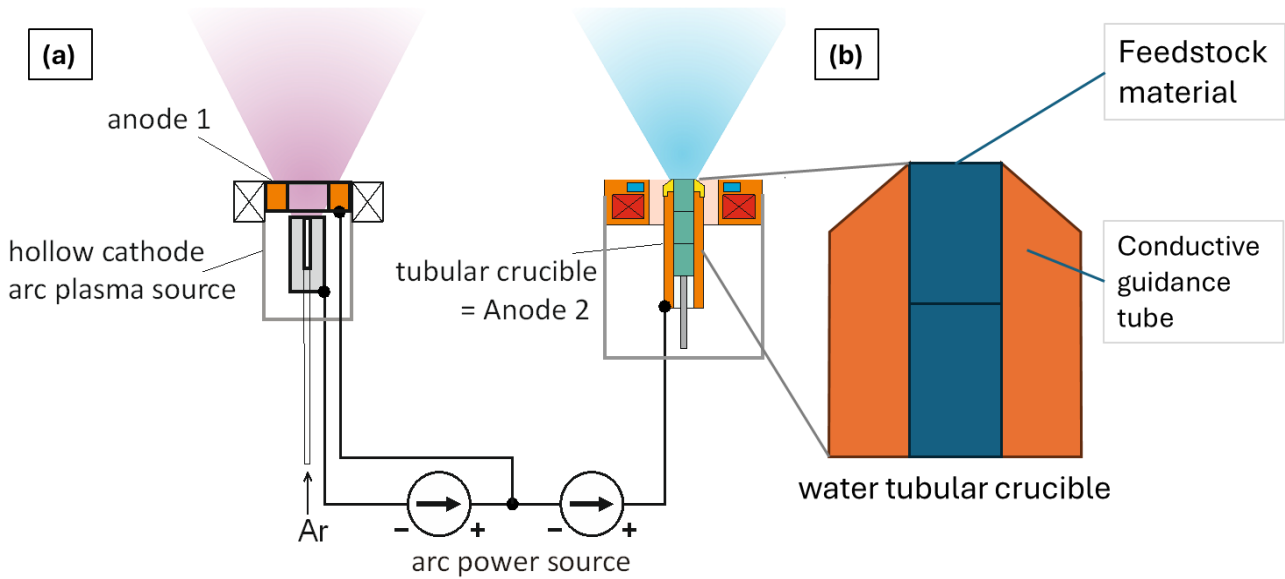


Figure 4: (a) Setup for anodic arc evaporation consisting of a hollow cathode plasma source and an evaporation device with tubular crucible and (b) redesign of the tubular crucible.

An evaluation of pros and cons of available coating facilities at FhG FEP was carried out (Table 2). For this the machines MAXI and VERSA have been considered, e.g., regarding feasible coating methods, process modes and conditions for an inert substrate handling. As a result, the VERSA tool has the best prerequisites but suffers from missing R2R-processing mode. Consequently, a draft design for a movable mini winding system was created. After adaption of the VERSA tool a R2R processing under inert conditions should be available.

Table 2: Aspects of various coating methods available at FhG FEP

Parameter	MAXI ²	VERSA ³
Coating methods	EB-PVD, Sputtering, Anodic Arc Evaporation, PE-CVD	
Processing	Inline	Batch
Mode	S2S ⁴ & R2R ⁵	S2S
Standard substrate size	500 mm x 500 mm (S2S) 300 mm x 1000m (R2R)	120 mm x 200 mm (S2S) (280 mm x 10 m, R2R after adaption)
Inert substrate handling	No	Yes

3.4. Soft sputtering of In-free TCOs.

Soft sputtering of indium-free TCO is being developed and optimized at TUD in the first 6 months. The first indium free TCOs have been processed using Radio Frequency (RF, 13.56 MHz) magnetron sputtering technique. A subtle dilution of the Ar carrier gas with oxygen during the sputter process improves the electrical and optical properties of SnO and FTO layers.

In addition, the concept of bi-layered has been further explored. In bilayer TCO stacks, even for low free charge carrier densities, superior hole mobilities with low sheet resistance and parasitic absorption can be achieved as the charge carrier transport is not limited by the grain boundary scattering mechanism of the integrated TCOs but due to its ionic impurity scattering. Playing with doping and crystallinity of

² <https://www.fep.fraunhofer.de/en/Kernkompetenzen/Anlagentechnik/maxi.html>

³ <https://www.fep.fraunhofer.de/en/Kernkompetenzen/Anlagentechnik/versa.html>

⁴ S2S – sheet-to-sheet

⁵ R2R – roll-to-roll

indium-free TCOs, bi-layered TCOs can be optimized for extra functionalities such as additional barriers for water ingress (lifetime extension) and wet-chemical processing (resilience in processing see T4.1). The first processed bilayers of FTO/SnO seem to have excellent optical and electrical properties to act as front window layer of solar cells. The properties of the chemical barrier functionality of the bilayer FTO/SnO still need to be tested.

Figure 5 shows the measured electrical mobilities μ versus the free charge carrier density N_e . The (μ , N_e)-values for IOH, ICO, i-ZnO are typical baseline values, which means that these TCO layers are a results of a first optimization cycle based on the processing and thermal annealing conditions. The (μ , N_e)-values for ITO and FTO represent TCO layers process under non-optimized sputter and thermal annealing conditions.

The processing conditions of the indium free i-SnO have been explored and wide range of The (μ , N_e)-values have been obtained. A combination of low pressures and a small partial pressure of oxygen gas in reference to the argon carrier gas results in materials with highest mobilities. Further optimization is under process. The (μ , N_e)-values for the FTO are indicative. These samples have been processed under conditions that the pressure was poorly controlled. An new attempt to process FTO with soft sputtering is currently carried out.

At TUDelft the following bi-layers have been tested using the material systems

- a) IOH/i-ZnO,
- b) ICO/i-ZnO,
- c) IOH/i-SnO_x (New- first attempt)
- d) FTO/i-SnO_x. (New-first attempt)

The crystal nature of the bilayer structure of the IOH/i-ZnO has so far been studied in more detail than the other bilayer structures. In figure 6 SEM cross section of IOH/i-ZnO bilayer is shown. The SEM cross section and top view images are taken to investigate the structural growth of bilayer. IOH exhibits a uniformly sputtered deposition on flat glass, reaching an approximate thickness of 70 nm. Above the IOH layer, a progressive increase in structural grains is observed with the growth of i-ZnO thickness, reaching 1.5 μm . This development results in the formation of larger grains on top of smaller i-ZnO grains (Figure 6.a and b).

Figures 6c and 6d demonstrate how the development of i-ZnO grains contributes to a surface with nano-featured characteristics in the bilayer design. In particular, Figure 6d highlights the presence of filaments within a single i-ZnO grain, indicating the preferred growth orientation of the material.

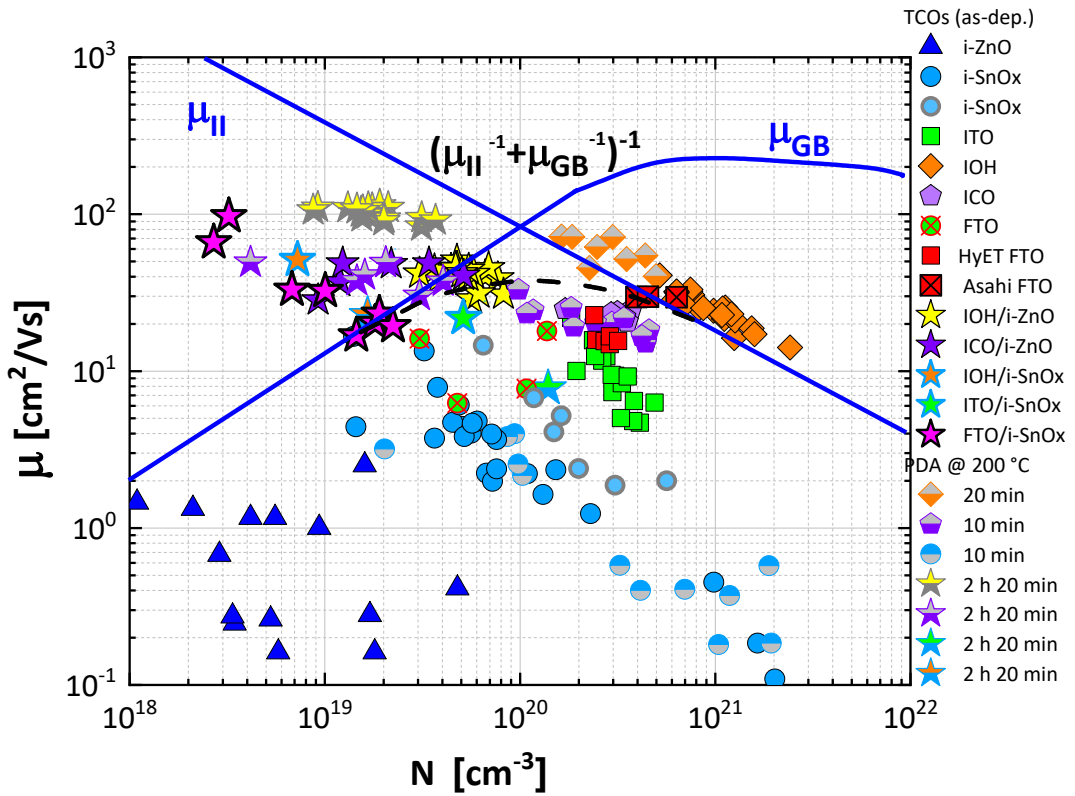


Figure 5. Overview of the electrical mobility versus the free charge carrier density of the current portfolio of TCO materials that can be processed at TUD. The blue lines represent the theoretical relation between the electrical mobility and the free charge carrier density for ZnO when the charge scattering mechanism is ruled by scattering at grain boundaries (GB) or by ionic impurities (II).

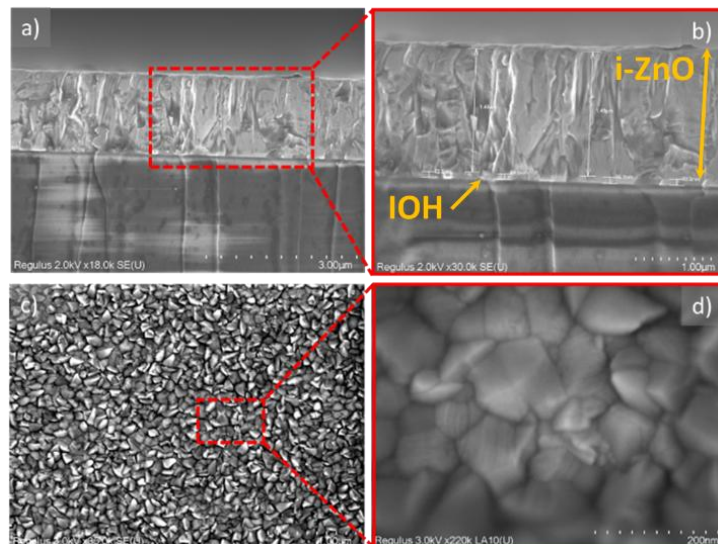


Figure 6: SEM cross-section images (a and b) and top-view images (c and d). Cross-section images reveal a bilayer with 70 nm IOH and 1.5 μm i-ZnO. The top-view images highlight sharp nano features from i-ZnO.

Figure 5 shows that (μ, Ne) -values for the bilayers are larger than what would be expected from the (μ, Ne) -values of the individual layers. The important result here is that the bilayers made of indium free TCOs, like the FTO/i-SnO bilayers follow the same trend and have excellent optical properties as shown in Figure 4. The further optimization of FTO and i-SnO and its corresponding bi-layers is currently carried out. The proposed understanding of the bilayer structure for the IOH/i-ZnO bilayer highlights the essential role of the interface between the Hydrogenated Indium Oxide and undoped Zinc Oxide layers in facilitating free carrier transport. Due to the substantial energy barrier presented by the grains in i-ZnO, free electrons primarily move in a transverse direction within this material. The crystallization of the IOH material after PDA treatment facilitates lateral transport of free carriers, providing an alternative and low resistive pathway at the interface with i-ZnO. Consequently, the grain boundaries are bypassed at the interface via the conductive IOH layer, indicating that free carrier lateral transport occurs within a certain penetration depth in the IOH material. The interpretation of the bilayer geometry is visually explained in Figure 7 in a simplified sketch. Whether this principle is universal for all bilayered TCOs is still under investigation.

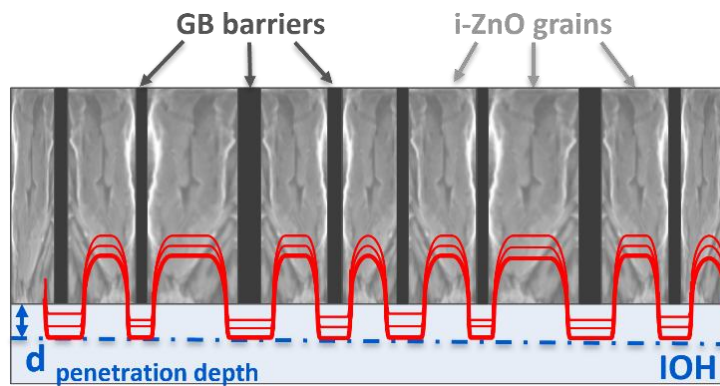


Figure 7: Simplified sketch illustrating the bilayer geometry and the role of the interface between IOH and i-ZnO layers in facilitating free carrier transport. Undoped Zinc Oxide grains and grain boundary (GB) barriers are depicted in light and dark grey respectively. Free charge carrier transport bypassing the grain boundaries is shown in red, while the penetration depth of this transport mechanism within the IOH layer is highlighted in blue.

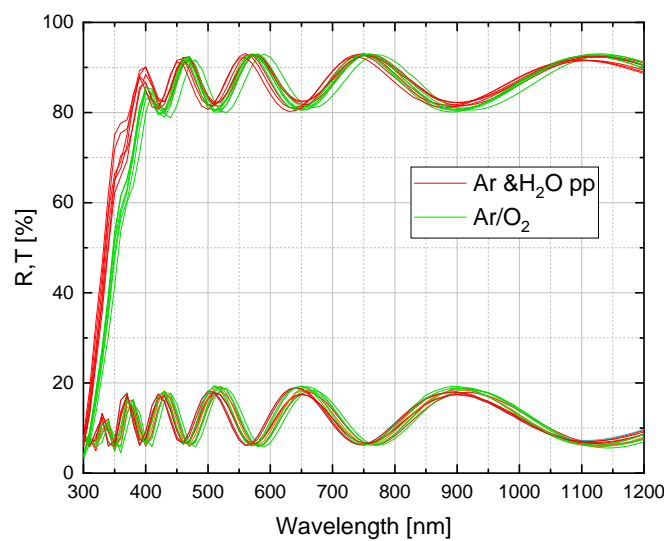


Figure 8: The transmission and reflection measurements on the first bi-layered FTO/i-SnO stacks processed.

4. Conclusions

NiOx has been selected as an attractive material as HTL for perovskite solar cells and modules. Sputtering might be an attractive approach for upscaling of deposition processes due to easy processing and excellent film thickness homogeneity to be reached. However, due to the classification of NiOx as CMR material a deeper risk analysis is necessary. Therefore, wet processing or alternative materials will be considered.

PCBM is the selected ETL and thick PCBM (~200 nm) are also considered for the additional blocking layer property. To achieve high performance fullerene-based diffusion blocking layers according to the requirements of the LUMINOSITY project we are evaluating the effect of meniscus coated N-DMBI doping on thick PCBM using FAPbI₃ perovskite formulation. Furthermore, alternative n-type doping materials will be studied in order to find the appropriate material that ensures a good compromise between stability and PCE.

A solution-processed protective buffer layer (PBL) to protect the perovskite stack from the sputtering of ITO transparent contact has been developed. The study encompasses a comparison of various buffer layer inks with variations in work function, viscosity, and solvent. Specifically, three different metal oxides nanoparticles, namely NP1, NP2, and NP3, were evaluated using different ink formulations. We found that NP2 demonstrated large compatibility with ITO better than the other two metal oxides. In particular, the use of NP2.2 allows to reach an efficiency of 18.1% similar to that of opaque cells with Cu contacts.

An evaluation of pros and cons of available coating facilities in the LUMINOSITY consortium was carried out. For this, the machines MAXI and VERSA have been considered, e.g., regarding feasible coating methods, process modes and conditions for an inert substrate handling. As a result, the VERSA tool has the best prerequisites but suffers from missing R2R-processing mode. Consequently, a draft design for a movable mini winding system was created. After adaptation of the VERSA tool a R2R processing under inert conditions should be available.

The first indium free TCOs have been processed using Radio Frequency (RF, 13.56 MHz) magnetron sputtering technique. A subtle dilution of the Ar carrier gas with oxygen during the sputter process improves the electrical and optical properties of SnO and FTO layers. The first processed bilayers of FTO/SnO seem to have excellent optical and electrical properties to act as front window layer of solar cells. The properties of the chemical barrier functionality of the bilayer FTO/SnO still need to be tested.

5. Degree of Progress

The deliverable is 100% fulfilled.

6. Dissemination level

The Deliverable D3.2 is public.